Electro-optic MMI coupler as wavelength demultiplexer for advanced SDM wireless-WDM optical signal converter

Mefina Yulias Rofianingrum[1,2], Yui Otagaki[1], Hiroshi Murata[1]
[1]High-Frequency Photonics Laboratory, Graduate School of Engineering, Mie University, Tsu-City, Japan
[2]Research Center for Photonics, National Research and Innovation Agency, Tangerang Selatan, Indonesia

Article Info

Article history:

Received Dec 31, 2023
Revised Mar 26, 2024
Accepted Mar 29, 2024

Keywords:

Electro-optic modulator
$LiNbO_3$
Multimode interference coupler
SDM-WDM converter
Wavelength demultiplexer

ABSTRACT

We report the design, fabrication, and experimental results of an optical wavelength demultiplexer for a new wireless-optical signal converter for Beyond-5G/6G mobile communication system. This optical wavelength demultiplexer is based on a lithium niobate ($LiNbO_3$) multimode interference (MMI) coupler and is intended to be applied in an advanced electro-optics modulator (EOM) with ability in converting the space division multiplexing (SDM) wireless-wavelength division multiplexing (WDM) optical signals. The designed MMI coupler displays a high splitting ratio over -13 dB in both O and L bands. The results from the experiments align well with the simulation. The utilization of the MMI coupler in EOM enables the direct conversion of SDM wireless signals to WDM optical signals, without any additional power supply. The modification of the characteristic of a constructed MMI coupler can be achieved by controlling of the applied voltage of the device.

Corresponding Author:

Mefina Yulias Rofianingrum
Research Center for Photonics, National Research and Innovation Agency,
Muncul, Setu, Tangerang Selatan, Banten, Indonesia.
Email: mefi001@brin.go.id

1. INTRODUCTION

The Beyond-5G/6G mobile communication system serves a dense population of phones and numerous gadgets. It must be also implemented with an average data transmission speed over 10 Gbit/s while maintaining low latency and sustained wireless connectivity. To attain over 10 Gbit/s transmission speed, an operational frequency should be chosen, taking millimeter wave (MMW) frequency allocation into account. However, the MMW wireless communication system encounters a drawback in the form of significant attenuation in metallic wires and free space [1]-[5]. Therefore, the implementation of radio over fiber (RoF) technology has become a feasible method to overcome the issues of MMW in communication systems. The RoF technology applies optical fiber to efficiently transmit microwave/MMW signals to remote antenna sites. Thus, it is composed of MMW domain and optical domain.

In MMW domain, the space division multiplexing (SDM) technology is used due to its advantage in constructing wireless networks with numerous terminals using a limited frequency band [6], [7]. While in optical domain, the utilization of the wavelength division multiplexing (WDM) technology in optical fiber networks has been recognized for its ability to enhance the capacity of current fiber optic networks without requiring the installation of extra fibers. Hence, the provision of flexible services and network management advantages can be realized [8]-[11]. To optimize the benefits and mitigate the drawbacks, the integration of the SDM and WDM techniques presents a compelling strategy for the development of mobile communication systems. To integrate these techniques, it is important to employ a device that enables the conversion of SDM wireless signals into WDM optical signals.

Extensive researches [12] have been conducted on electro optics modulators (EOMs) utilizing lithium niobate ($LiNbO_3$) as the base material. These modulators have demonstrated the ability to efficiently convert wireless MMW signals into optical signals, exhibiting exceptional modulation characteristics. The $LiNbO_3$ EOMs exhibit high-speed and broadband operation, surpassing 100 GHz. Moreover, they offer pure optical phase modulation without any chirping effects, wide operational optical wavelength ranges, and demonstrate stability and reliability [12], [13]. The research on the integration of the antenna coupled electrode (ACE) with a $LiNbO_3$ based EOM has been conducted to explore its benefits, such as direct conversion and the absence of an external power supply [7], [14]. The utilization of polarization-reversed structure combination in EOMs has also been employed to obtain directivity control in signal conversion. Hence, the discrimination of MMW signals based on their irradiation angles can be accomplished [7].

Meanwhile, wavelength demultiplexers have crucial functions in optical transmission networks [15]. Various devices have been presented to fulfill this purpose, including Mach-Zehnder interferometers [16]-[18], Y-branch devices [19], [20], and multimode interference (MMI) couplers [21]–[24]. In this regard, MMI-based devices are promising options because of their wide range of advantageous properties, such as their compact size, high optical bandwidth, and ease of fabrication [24]. This letter reports the design and fabrication of MMI coupler using z-cut $LiNbO_3$ crystal. The designed MMI coupler will be utilized in the EOM to enable the direct conversion of the SDM wireless signals to the WDM optical signals, without any additional power supply.

2. PROPOSED DEVICE

The novel SDM wireless-WDM optical signals conversion device was proposed using combination of ACE, polarization-reversed structure and MMI couplers in $LiNbO_3$-based EOM [25] as shown in Figure 1. The ACE is a combination of a dual set of patch antennas and a resonant electrode that are connected with a microstrip line. The ACE is positioned between two layers: SiO_2, with a thickness of approximately 20 μm, serving as a low-*k* substrate, and a thin crystal film of $LiNbO_3$, with a thickness of around 10 μm. The utilization of a polarization-reversed structure on the $LiNbO_3$ crystal film, along with optical channel waveguides, enables discrimination of wireless signals based on the angles of irradiation.

The MMI couplers provide the purpose of demultiplexing and multiplexing the input optical signal. The input optical signal is divided by the first MMI coupler, acting as a wavelength demultiplexer. Upon irradiation of wireless signals onto the device, the patch antenna array receives the signals and subsequently transfers them to the resonant electrodes through the feeding lines. This process induces standing-wave electric fields along the electrodes. Since the optical waveguide ports are located just onto the electrodes, the optical signal propagating in each the optical waveguides are modulated and the synthesis of the received signals are obtained through the successive optical modulation by the ACE array. The condition of the synthesized signals is altered in accordance with the polarization-reversed structure pattern. Thus, the optical signals propagating in each port are modulated by different SDM wireless signals. Finally, the signals combined by the second MMI coupler and the WDM optical signals are obtained. Hence, the utilization of a complex signal synthesis circuit to fine-tune signal amplitudes and phases is deemed unnecessary. Therefore, by merely irradiating the specifically designed SDM wireless signals to the device, it is possible to acquire the WDM optical signals without the need for any additional power supply.

The MMI coupler is composed of single-mode channel waveguides and a multimode channel waveguide, as illustrated in Figure 2. Figure 2(a) shows the schematic diagram of the developed MMI coupler, whereas Figure 2(b) illustrates the cross-sectional diagram. An important process of determining the effective refractive index of the optical channel waveguide for the design of the MMI coupler is the utilization of the effective index method (EIM). In this approach, the SiO_2 and the $LiNbO_3$ layer act as the cladding layer, and the annealed proton exchanged (APE) layer acts as the core layer of the waveguide. The coupler is designed to divide the input optical signal into two different wavelengths, specifically 1310 nm and 1582 nm. The principle underlying the MMI device is the self-imaging phenomenon, in which the input optical signal at each wavelength is regularly replicated with a beat length of L_π, where:

$$L_\pi \cong \frac{4N_{eff}{W_e}^2}{3\lambda} \quad (1)$$

N_{eff} represents the effective index, W_e is the effective width, and λ is the optical wavelength [24]. The calculation of the length of the multi-mode channel waveguide (L_{mmi}) is necessary to achieve wavelength division in the MMI coupler, as described by the (2).

$$L_{mmi} = pL_{\lambda_1} = (p+1)L_{\lambda_2} \quad (2)$$

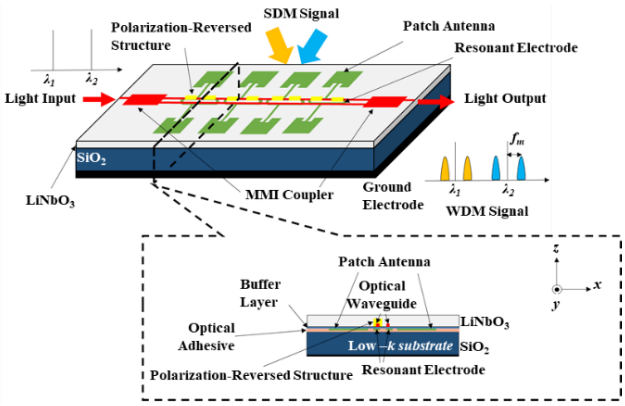

Figure 1. SDM wireless-WDM optical signal converter

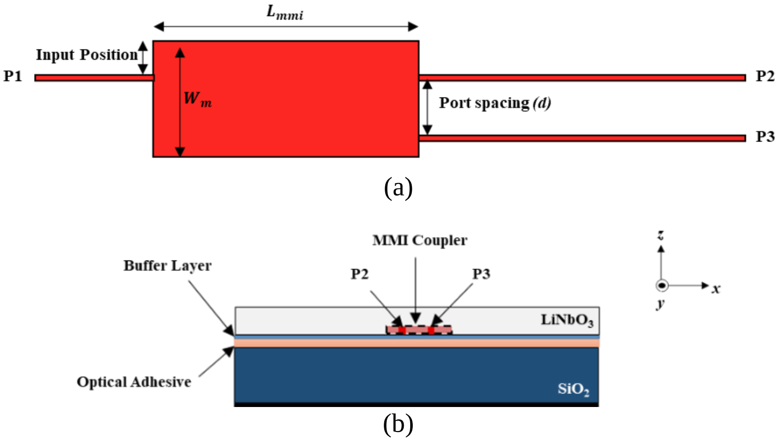

Figure 2. Model of MMI coupler; (a) schematic diagram of MMI coupler and (b) cross-section of MMI coupler's schematic diagram

The value p represents the order number. Figure 3 demonstrates the utilization of a BPM simulation to build and assess the MMI coupler, resulting in the achievement of wavelength-selective output operation. The dimensions of the multi-mode optical channel waveguide are specified as a width of 40 µm and a length of 11.3 mm. The input position is set at 7µm, and the port spacing (d) is defined as 22 µm. The dimensions of the single-mode waveguides are set with a width of 3 µm and a depth of 3.45µm. The simulation parameters for the MMI coupler are detailed in Table 1. In Figure 3, it is apparent that most of the input signal goes to a single selective port.

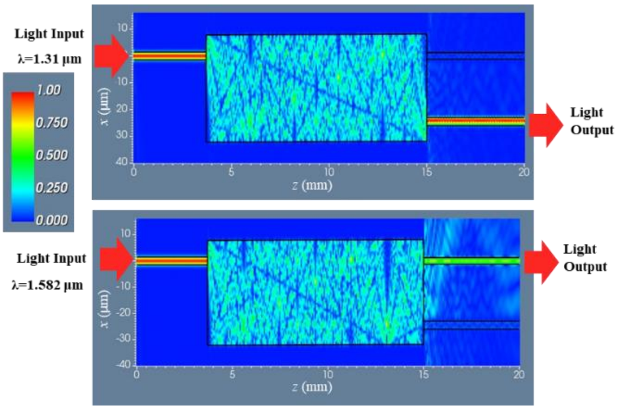

Figure 3. BPM analysis of MMI coupler

Table 1. Parameters of the designed MMI coupler

Parameters	Dimensions
MMI coupler width (W_m)	40 µm
MMI coupler length (L_{mmi})	11.3 mm
Single mode waveguide (P1, P2, P3) width	3 µm
Port separation (d)	22 µm
Input port (P1) position from edge	7 µm
MMI coupler depth	3.45 µm
n_{eff}	2.266 (at 1.31 µm); 2.265 (at 1.582 µm)
$n_{clad1\ (SiO_2)}$	2.145 (at 1.31 µm); 2.137 (at 1.582 µm)
$n_{clad2\ (LiNbO_3)}$	2.275 (at 1.31 µm); 2.267 (at 1.582 µm)

Figure 4 illustrates the power splitting ratio between two output ports in relation to the input optical wavelength. Figure 4(a) displays the power splitting ratio for P_3, while Figure 4(b) exhibits the power splitting ratio for P_2. The designed MMI coupler exhibits the maximum splitting ratio at a wavelength of 1310 nm at P3, and at a wavelength of 1582 nm at P2. The corresponding power splitting ratios are measured to be -14.43 dB and -13.47 dB, respectively. The optical bandwidth of port 3 (P3) is relatively narrower than that of port 2 (P2). The current setup of the MMI coupler offers optical bandwidths of 2 nm for P3 and 8 nm for P2.

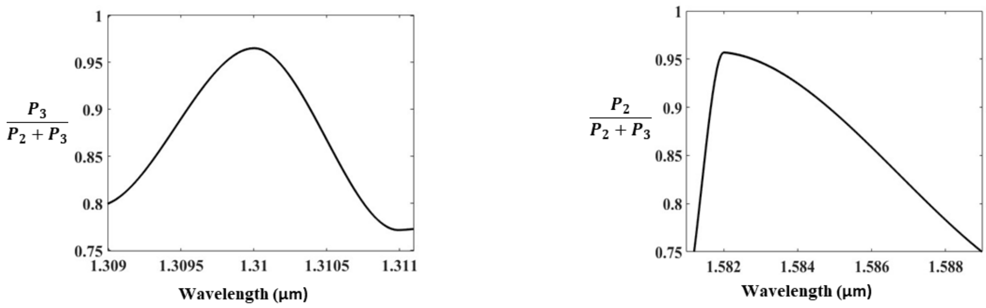

(a) (b)

Figure 4. Power splitting ratio in relation to the input optical wavelength: (a) for P_3 and (b) for P_2

3. METHOD

The designed MMI coupler was fabricated on a z-cut $LiNbO_3$ wafer using the APE method. Various fabrication conditions, including as proton exchange temperature, exchange time, annealing temperature, and annealing time, have an impact on the dimensions of the fabricated coupler, such as its depth. Consequently, the acquired effective index will be influenced, thereby impacting the beat length. Hence, the choice of the fabrication conditions has a significant role in modifying the performance of the MMI coupler [26]. The proton-exchange process was conducted at the temperature of 240 °C for the duration of 6 hours. Subsequently, the annealing process was conducted at the temperature of 350 °C for the duration of one hour. Figure 5 portrays the microscopic image of the fabricated MMI coupler. Figure 5(a) displays the microscopic image of the input region of the MMI coupler, whereas Figure 5(b) exhibits the output region of the MMI coupler.

Figure 6 shows experimental demonstrations of the performance of the fabricated MMI coupler. The laser optical signal was transferred through the input port using a fiber coupler and then transmitted to the output port. The transmitted signal is coupled to the infrared camera by using an objective lens.

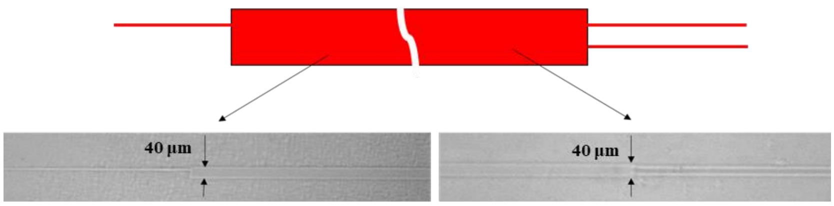

(a) (b)

Figure 5. Microscopic images of fabricated MMI coupler: (a) input region image and (b) output region image

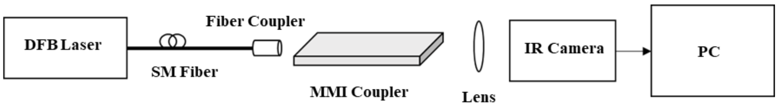

Figure 6. Experimental set up

4. RESULTS AND DISCUSSION

The measured near field images of the output optical signals obtained from the experiment are shown in Figure 7. The result obtained at input wavelength 1.31 μm is depicted in Figure 7(a), while the result obtained at 1.582 μm is illustrated in Figure 7(b). The optical intensity distributions along the horizontal directions, which are obtained from the output near field images are also depicted in Figure 7. These distributions correspond with the output power. Figure 8 illustrates the comparison of the normalized power output between the simulation and experiment, in relation to the input optical wavelength. Figure 8(a) illustrates the comparison for P_3, while Figure 8(b) depicts the comparison for P_2. Based on Figures 8(a) and 8(b), it is evident that the experimental results have good agreement with the simulation.

The MMI coupler will be applied in the EOM based on $LiNbO_3$. This EOM employs the Pockels effect, which induces a change in the refractive index of the $LiNbO_3$ crystal. The induced index change in TM-mode can be described using (3):

$$\Delta n = \frac{1}{2} {n_e}^3 \gamma_{33} E \quad (3)$$

where n_e represents the extraordinary refractive index, γ_{33} denoted the Pockels coefficient and E is the applied electric field [12]. The fundamental principle underlying EOM is the induction of a phase shift that is depended on the applied voltage. The optical and electrical fields must be oriented with respect to the crystal orientation with the highest EO effect.

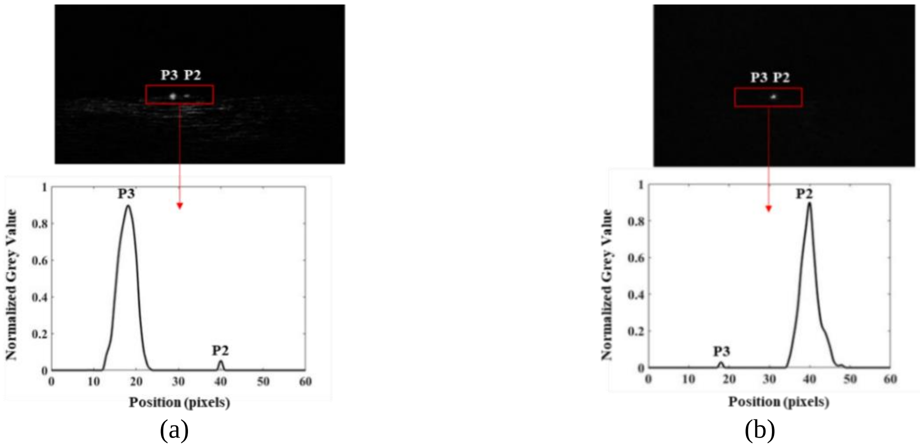

Figure 7. Measured near field patterns and analyzed intensity distributions along the horizontal direction; (a) 1.31 μm and (b) 1.582 μm

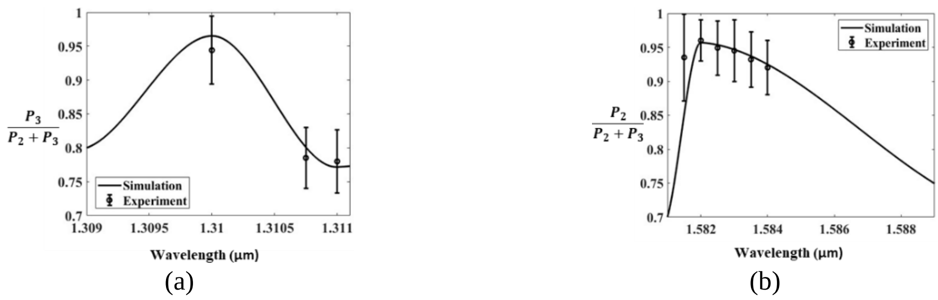

Figure 8. Comparison of power splitting ratio between simulation and experiment in relation to the input optical wavelength for; (a) P_3 and (b) P_2

Therefore, two electrodes between the multimode waveguide of the MMI coupler can be utilized as shown in Figure 9, and the application of a designated voltage to induce a change in the effective refractive index, implementing the Pockels effect. As a result, the characteristics of the MMI coupler will be altered by the electric field that is applied. Consequently, the properties of the MMI coupler will undergo modification of the applied electric field, which arises from the Pockels effect. The operation wavelength of the MMI coupler will also be subject to change when utilizing the equation. Figure 10 illustrates the relationship between the power splitting ratio and input wavelength, considering various applied voltages, while assuming a 40 μm gap between the electrodes (D). Figure 10(a) displays the power splitting ratio for P_3, while Figure 10(b) exhibits the power splitting ratio for P_2. Based on the calculated results presented in Figures 10(a) and 10(b), it is evident that the wavelength peak undergoes a shift of approximately 9 nm for every 5 V of applied voltage. Hence, it is evident that the tunability of the MMI coupler can be achieved by altering the applied voltage.

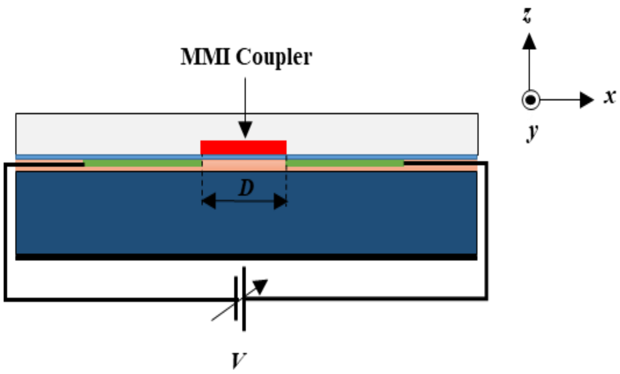

Figure 9. Cross-sectional view of structure of guided-wave EOM

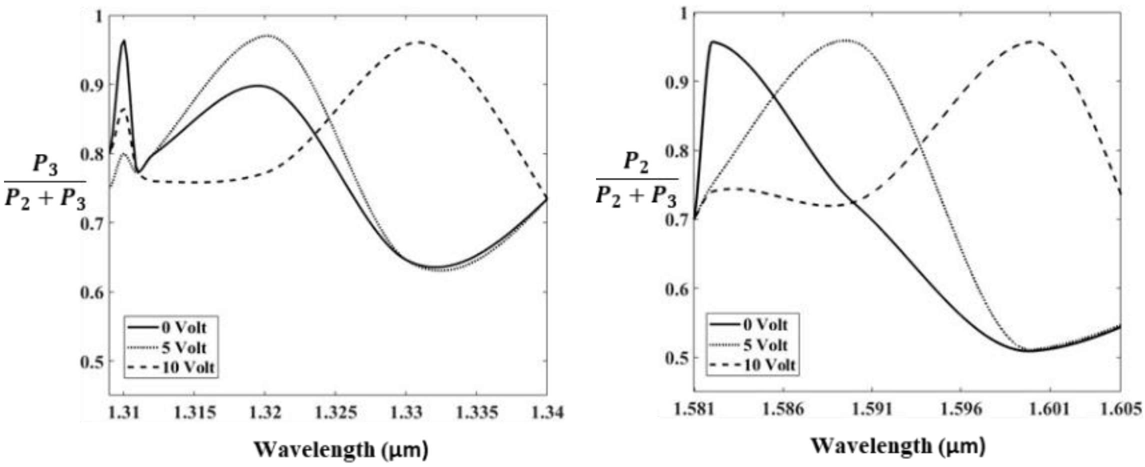

(a) (b)

Figure 10. Power splitting ratio as function of wavelength with different applied voltage for: (a) P_3 and (b) P_2

5. CONCLUSION

In conclusion, the design and fabrication outcome of a wavelength demultiplexer utilizing an MMI coupler implemented with a z-cut $LiNbO_3$ crystal has been successfully demonstrated. The designed MMI coupler displays a high splitting ratio over -13 dB in both the O and L bands. The results from the experiments align well with the simulation. The utilization of the MMI coupler in EOM enables the direct conversion of SDM wireless signals to WDM optical signals, without any additional power supply. The modification of the characteristic of a constructed MMI coupler can be achieved by controlling of the applied voltage of the device.

ACKNOWLEDGEMENTS

This work was supported in part by the research and development project (JPJ012368C00501) entitled with "THz and optical wireless aggregation research and development for B5G (Toward-B5G)" from NICT, Japan.

REFERENCES

[1] A. Sufyan, K. B. Khan, O. A. Khashan, T. Mir, and U. Mir, "From 5G to beyond 5G: A Comprehensive Survey of Wireless Network Evolution, Challenges, and Promising Technologies," *Electronics*, vol. 12, no. 10, Jan. 2023, doi: 10.3390/electronics12102200.
[2] T. Nagatsuma and A. Hirata, "10-Gbit/s Wireless Link Technology Using the 120GHz Band Letters," vol. 2, no. 11, Nov. 2004.
[3] R. Baldemair *et al.*, "Evolving Wireless Communications: Addressing the Challenges and Expectations of the Future," *IEEE Vehicular Technology Magazine*, vol. 8, no. 1, pp. 24–30, Mar. 2013, doi: 10.1109/MVT.2012.2234051.
[4] M. Marcus and B. Pattan, "Millimeter wave propagation: spectrum management implications," *IEEE Microwave Magazine*, vol. 6, no. 2, pp. 54–62, Jun. 2005, doi: 10.1109/MMW.2005.1491267.
[5] B. K. J. Al-Shammari, I. Hburi, H. R. Idan, and H. F. Khazaal, "An Overview of mmWave Communications for 5G," in *2021 International Conference on Communication & Information Technology (ICICT)*, Basrah, Iraq, pp. 133–139, Jun. 2021, doi: 10.1109/ICICT52195.2021.9568459.
[6] A. Dixit, "Architectures and Algorithms for Radio-Over-Fiber Networks," *Journal of Optical Communications and Networking*, vol. 10, no. 5, pp. 535–544, May 2018, doi: 10.1364/JOCN.10.000535.
[7] H. Murata, R. Miyanaka, and Y. Okamura, "Wireless space-division-multiplexed signal discrimination device using electro-optic modulator with antenna-coupled electrodes and polarization-reversed structures," *International Journal of Microwave and Wireless Technologies*, vol. 4, no. 3, pp. 399–405, Jun. 2012, doi: 10.1017/S175907871200030X.
[8] S. Okamoto *et al.*, "A Study on the Effect of Ultra-Wide Band WDM on Optical Transmission Systems," *Journal of Lightwave Technology*, vol. 38, no. 5, pp. 1061–1070, Mar. 2020, doi: 10.1109/JLT.2019.2962178.
[9] T. Jose, V. D. John, and S. Pandiaraj, "Performance analysis of WDM MIMO RoFSO links for 5G applications," *TELKOMNIKA Telecommunication, Computing, Electronics and Control*, vol. 20, no. 2, pp. 260-267, Apr. 2022, doi: 10.12928/telkomnika.v20i2.22829.
[10] G. Pandey, A. Choudhary, and A. Dixit, "Wavelength Division Multiplexed Radio Over Fiber Links for 5G Fronthaul Networks," *IEEE Journal on Selected Areas in Communications*, vol. 39, no. 9, pp. 2789–2803, Sep. 2021, doi: 10.1109/JSAC.2021.3064654.
[11] P. Winzer, "Optical networking beyond WDM," *IEEE Photonics Journal*, vol. 4, no. 2, pp. 647–651, Apr. 2012, doi: 10.1109/JPHOT.*2012*.2189379.
[12] E. L. Wooten *et al.*, "A review of lithium niobate modulators for fiber-optic communications systems," *IEEE Journal of Selected Topics in Quantum Electronics*, vol. 6, no. 1, pp. 69–82, Jan. 2000, doi: 10.1109/2944.826874.
[13] M. Li, J. Ling, Y. He, U. A. Javid, S. Xue, and Q. Lin, "Lithium niobate photonic-crystal electro-optic modulator," *nature communications*, vol. 11, no. 1, Aug. 2020, doi: 10.1038/s41467-020-17950-7.
[14] H. Murata, "Millimeter-Wave-Band Electro-Optic Modulators Using Antenna-Coupled Electrodes for Microwave Photonic Applications," *Journal of Lightwave Technology*, vol. 38, no. 19, pp. 5485–5491, Oct. 2020, doi: 10.1109/JLT.2020.3004176.
[15] Y. Calvin Si and Y. Cheng, "Chapter 3 - Optical Multiplexer/Demultiplexer: Discrete," in *WDM Technologies*, pp. 39–78. doi: 10.1016/B978-012225262-4/50005-2.
[16] Y. Li *et al.*, "High-Performance Mach–Zehnder Modulator Based on Thin-Film Lithium Niobate with Low Voltage-Length Product," *ACS* Omega, vol. 8, no. 10, pp. 9644-9651, Mar. 2023, doi: 10.1021/acsomega.3c00310.
[17] H. Xu, L. Liu, and Y. Shi, "Polarization-insensitive four-channel coarse wavelength-division (de)multiplexer based on Mach–Zehnder interferometers with bent directional couplers and polarization rotators," *Optics Letters*, vol. 43, no. 7, pp. 1483–1486, Apr. 2018, doi: 10.1364/OL.43.001483.
[18] S. Ohta *et al.*, "Si-based Mach-Zehnder wavelength/mode multi/demultiplexer for a WDM/MDM transmission system," *Optics Express*, vol. 26, no. 12, pp. 15211–15220, Jun. 2018, doi: 10.1364/OE.26.015211.
[19] C. Sun, J. Zhao, Z. Wang, L. Du, and W. Huang, "Broadband and high uniformity Y junction optical beam splitter with multimode tapered branch," *Optik*, vol. 180, pp. 866–872, Feb. 2019, doi: 10.1016/j.ijleo.2018.12.013.
[20] Y. Xu, W. Zhou, K. Chen, and X. Huang, "Y-branch wavelength demultiplexer based on topological valley photonic crystals," *Optics & Laser Technology*, vol. 155, p. 108422, Nov. 2022, doi: 10.1016/j.optlastec.2022.108422.
[21] J. Menahem and D. Malka, "1 × 4 Wavelength Demultiplexer C-Band Using Cascaded Multimode Interference on SiN Buried Waveguide Structure," *Materials*, vol. 15, no. 14, Jan. 2022, doi: 10.3390/ma15145067.
[22] S.-L. Tsao, H.-C. Guo, and C.-W. Tsai, "A novel 1×2 single-mode 1300/1550 nm wavelength division multiplexer with output facet-tilted MMI waveguide," *Optics Communications*, vol. 232, no. 1-6, pp. 371–379, Mar. 2004, doi: 10.1016/j.optcom.2003.12.082.
[23] J. Xiao, X. Liu, and X. Sun, "Design of an ultracompact MMI wavelength demultiplexer in slot waveguide structures," *Optics Express*, vol. 15, no. 13, pp. 8300–8308, Jun. 2007, doi: 10.1364/OE.15.008300.
[24] L. B. Soldano and E. C. M. Pennings, "Optical multi-mode interference devices based on self-imaging: principles and applications," *Journal of Lightwave Technology*, vol. 13, no. 4, pp. 615–627, Apr. 1995, doi: 10.1109/50.372474.
[25] M. Y. Rofianingrum, Y. Otagaki, and H. Murata, "Novel Electro-Optic Modulator Using Antenna-Coupled Electrode and MMI coupler for Converting SDM Mobile Wireless Signals to WDM Optical Signals," *International Conference on Emerging Technologies for Communications*, vol. 72, no. S1-4, Nov. 2022, doi: 10.34385/proc.72.S1-4.
[26] K. Tada, T. Murai, T. Nakabayashi, T. Iwashima, and T. Ishlkawa, "Fabrication of $LiTaO_3$ Optical Waveguide by H^+ Exchange Method," *Japanese Journal of Applied Physics*, vol. 26, no. 3R, p. 503, Mar. 1987, doi: 10.1143/JJAP.26.503.

BIOGRAPHIES OF AUTHORS

Mefina Yulias Rofianingrum received the Bachelor degree in Physics in 2013, and the Master's degree in Physics Engineering in 2016 from the Institute Technology of Sepuluh Nopember (ITS), Surabaya, Indonesia. She is currently graduate student of engineering in Mie University, Japan and a researcher in National Research and Innovation Agency, Indonesia. Her current research interests include 5G/ Beyond 5G mobile systems, photonics and related applications in fiber optic sensor. She is member of the IEEE, OSA and IEICE. She can be contacted at email: mefi001@brin.go.id and 421db01@m.mie-u.ac.jp.

Yui Otagaki received the B.E. and M.E. degrees in Electrical Engineering from Osaka University, Osaka, Japan, and a Ph.D. degree in Engineering from King's College London, University of London, UK. She is currently an assistant professor in the Graduate School of Engineering, Mie University, Tsu, Japan. Her research interests include 5G/ Beyond 5G mobile systems, microwave photonics and related applications in remote sensing, and Nuclear Quadrupole Resonance. She can be contacted at email: otagaki@elec.mie-u.ac.jp.

Hiroshi Murata received the B.Eng., M.Eng., and D.Eng. degrees in Electrical Engineering from Osaka University, Osaka, Japan in 1988, 1990, and 1998, respectively, for studies on the guided-wave systems with third-order optical nonlinearity and their applications to all-optical functional devices. In 1991, he joined the Department of Electrical Engineering, Faculty of Engineering Science, Osaka University. In 2018, he moved to the Area of Electric Engineering, Graduate School of Engineering, Mie University, Tsu, Japan, where is he is currently a Professor. He is the author and coauthor of more than 260 scientific publications in his areas of research, and holds various patents too. His research interests include 5G/Beyond 5G mobile systems, microwave photonics, integrated optics and nonlinear optics. He is an Associate Editor of the IEICE Electronics Express (ELEX) in the IEICE, Japan, in 2009-2012 and was the Guest Editor of the Journal Advances in Optoelectronics in the special issue: "progress in domain-engineered photonic materials", in 2007–2008. He is also a member of the EuMA, the IEEE Photonics and MTT societies, the OSA, the JSAP, the IEICE, and the Laser Society of Japan. He was the recipient of the 35th European Microwave Conference Microwave Prize in 2005, the IEEE Photonics Global Singapore Best Paper Award in 2008, the 2017 Micro-Optics Conference Paper Award in 2017, and the IEC Award in 2017. He can be contacted at email: murata@elec.mie-u.ac.jp.